S6 kinase localizes to the presynaptic active zone and functions with PDK1 to control synapse development

Ling Cheng, Cody Locke, and Graeme W. Davis

Department of Biochemistry and Biophysics, University of California, San Francisco, San Francisco, CA 94158

The dimensions of neuronal dendrites, axons, and synaptic terminals are reproducibly specified for each neuron type, yet it remains unknown how these structures acquire their precise dimensions of length and diameter. Similarly, it remains unknown how active zone number and synaptic strength are specified relative the precise dimensions of presynaptic boutons. In this paper, we demonstrate that S6 kinase (S6K) localizes to the presynaptic active zone. Specifically, S6K colocalizes with the presynaptic protein Bruchpilot (Brp) and requires Brp for active zone localization. We then provide evidence that S6K functions downstream of presynaptic PDK1 to control synaptic bouton size, active zone number, and synaptic function without influencing presynaptic bouton number. We further demonstrate that PDK1 is also a presynaptic protein, though it is distributed more broadly. We present a model in which synaptic S6K responds to local extracellular nutrient and growth factor signaling at the synapse to modulate developmental size specification, including cell size, bouton size, active zone number, and neurotransmitter release.

Introduction

The mechanisms that specify neuronal size and shape are essential to the generation of robust neural circuitry. Axon diameter, dendrite diameter, the size of a dendritic field, and the area of the presynaptic nerve terminal are all reproducibly specified for a given cell type. The size and complexity of a neuron far exceeds that of any other cell type, suggesting that there may be unique solutions to the challenge of controlling and coordinating the growth of the many different and distinct features of neuronal architecture. Specification of neuronal dimension is further complicated because it is intimately associated with the electrochemical function of the neuron. Indeed, a specific form of neuronal growth, isoelectronic growth, has been observed in both invertebrates and vertebrates in which dendrite diameter grows precisely as the square of dendrite length, thereby maintaining the cable properties of individual dendrites (Hill et al., 1994). This type of growth is fundamentally different from most types of neuronal growth that are characterized experimentally, including axon extension, dendrite branching, spine formation, and synapse expansion. It remains unknown how the dimensions of individual neuronal compartments can be precisely specified and how these growth-related parameters are coordinated with neuronal function. Mechanistically, very few studies report the identification of genes that specifically control neuronal dimensions without otherwise perturbing the ability of these structures to form properly.

Candidates for the control of neuronal dimension are genes associated with the regulation of cell size, including mammalian target of rapamycin, PDK1, and S6 kinase (S6K). S6K is necessary for long-term facilitation (Weatherill et al., 2010), the early phase of long-term potentiation (Antion et al., 2008), learning (Antion et al., 2008), and activity-dependent neuronal sprouting during epilepsy (Buckmaster et al., 2009). S6K also influences the growth of dendritic arbors in cultured hippocampal neurons (Jaworski et al., 2005). However, there are conflicting studies regarding whether S6K influences bouton number at the *Drosophila melanogaster* neuromuscular junction (NMJ; Knox et al., 2007; Howlett et al., 2008; Shen and Ganetzky, 2009).

Correspondence to Graeme W. Davis: Graeme.davis@ucsf.edu

Abbreviations used in this paper: Brp, Bruchpilot; EPSP, excitatory postsynaptic potential; mEPSP, miniature EPSP; NMJ, neuromuscular junction; PhTx, philanthotoxin; S6K, S6 kinase.

The Rockefeller University Press $30.00
J. Cell Biol. Vol. 194 No. 6 921–935
www.jcb.org/cgi/doi/10.1083/jcb.201101042

Results

Here, we take advantage of a previously characterized mutation in *Drosophila S6K*. The $S6K^{l\text{-}1}$ mutation deletes part of the first gene exon including part of the catalytic domain and is believed to be to a strong hypomorphic or null mutation (Montagne et al., 1999). We first confirm that *S6K* controls cell size in the *Drosophila* nervous system, consistent with and extending prior observations (Howlett et al., 2008; Shen and Ganetzky, 2009). Loss of *S6K* results in a smaller ventral ganglion, smaller motoneuron cell bodies, and smaller motor axons (Fig. S1 and not depicted). However, the gross organization of the central and peripheral nervous systems appears normal (Fig. S1). Thus, consistent with data in *Drosophila* and mammals, *S6K* is necessary for the control of cell size in the nervous system.

S6K controls bouton size without altering bouton number

Here, we find that *S6K* mutations do not alter synaptic bouton number at the *Drosophila* NMJ (Fig. 1), consistent with previous work (Knox et al., 2007; Shen and Ganetzky, 2009). Given that S6K regulates cell size in multiple tissues, we also examined the size of muscle fibers in *S6K* mutants and found a trend toward a decrease in muscle size, but the change was not statistically significant (control: 0.0433 mm^2; $S6K^{l\text{-}1}/df$: 0.0403 mm^2; $P > 0.05$). In addition, muscle input resistance, measured electrophysiologically, was used as a quantitative and independent measurement to assess changes in muscle size. We find a small change in muscle input resistance in *S6K* mutants (see section regarding synaptic electrophysiology). It appears that loss of S6K does not strongly influence muscle size, though it is possible that other developmental mechanisms are able to compensate for the loss of S6K in the *Drosophila* muscle. To adjust for potential differences in muscle size, we also normalized bouton number to muscle area and found that the normalized bouton number was not significantly different when comparing *S6K* mutants with wild type (wild type: 544.89 boutons/mm^2; $S6K^{l\text{-}1}/df$: 582.52 boutons/mm^2; $P > 0.05$). However, we find that synaptic bouton size is dramatically altered. In the *S6K* mutant, mean bouton size is ~40% smaller than wild type (Fig. 1, B and G). Bouton size is determined by measuring the area of individual synaptic boutons in a 2D projection of a 3D confocal image stack, staining the NMJ using the membrane marker anti-HRP combined with the presynaptic vesicle-associated protein antisynapsin. Thus, S6K regulates bouton size without altering bouton number or muscle size.

Next, we sought to determine whether S6K is required pre- or postsynaptically for the regulation of bouton size. To do so, we expressed a *UAS-S6K* transgene in either neurons or muscle using tissue-specific GAL4 drivers. The decrease in bouton size was fully rescued by neuronal expression of *UAS-S6K*, with either the panneuronal driver *C155-Gal4* or the motoneuron-specific driver *OK371-Gal4* (Fig. 1, C and G). Muscle-specific expression using *BG57-Gal4* failed to rescue the decrease in bouton size (Fig. 1, D and G). We conclude that presynaptic S6K is essential for the regulation of bouton size.

We then asked whether S6K activity is required for the control of synaptic bouton size. The kinase-dead $UAS\text{-}S6K^{KQ}$ mutates a conserved lysine residue in the ATP binding site and renders the kinase catalytically inactive (Barcelo and Stewart, 2002). The hyperactive $UAS\text{-}S6K^{STDETE}$ substitutes three conserved S6K phosphorylation sites at the autoinhibitory domain and the linker region to acidic residues and has higher levels of basal activity (Barcelo and Stewart, 2002). We drove the expression of both constructs with the neuronal driver *C155-Gal4* and found that the kinase-dead $UAS\text{-}S6K^{KQ}$ failed to rescue any defects in bouton size (Fig. 1, F and I). In contrast, the hyperactive $UAS\text{-}S6K^{STDETE}$ not only rescued the decrease in bouton size but also caused an increase in bouton size. The bouton size of $UAS\text{-}S6K^{STDETE}$ rescue was 175% of control (Fig. 1, E and I). Again, bouton number was unchanged in all conditions (control: 23.26 boutons/synapse; $UAS\text{-}S6K^{KQ}$: 24.51 boutons/synapse; $UAS\text{-}S6K^{STDETE}$: 22.06 boutons/synapse; $P > 0.05$ compared with control). We also obtained similar results when using the motoneuron-specific driver *OK371-Gal4* (Fig. 1), confirming that these effects are independent of the exact neuronal driver that was used. From these data, we conclude the kinase activity of S6K is essential for the regulation of bouton size. Furthermore, because the hyperactive S6K transgene enhances bouton size without a change in bouton number, we conclude that S6K is both necessary and sufficient to control the dimension of synaptic boutons at the NMJ independent of bouton formation.

S6K localizes to the presynaptic active zone via a Brp-dependent mechanism

To characterize the localization of S6K, we fused a 3×FLAG tag to the N terminus of S6K and generated *UAS-3×FLAG-S6K* transgenic flies. When driven with the motoneuron-specific driver *OK371-Gal4*, S6K was detected in cell bodies and diffusely within motoneuron axons. At the synapse, S6K was present in a highly punctate pattern (Fig. 2 A), reminiscent of the active zone marker Bruchpilot (Brp; Kittel et al., 2006; Wagh et al., 2006). Subsequently, we discovered that FLAG-tagged S6K and Brp colocalize throughout the NMJ (Fig. 2 A). In addition, FLAG-tagged S6K puncta are precisely opposed by antibody staining that recognizes the postsynaptic glutamate receptor GluRIIC (Fig. 2 B). Finally, there is little overlap with the periactive zone marker Dap160 (Fig. 2 C). In contrast, when S6K expression is driven using the muscle-specific driver *BG57-Gal4*, S6K staining was found throughout muscle fibers, with only a slight enrichment around the subsynaptic reticulum (Fig. S2 A). Collectively, we conclude that S6K localizes to the presynaptic active zone, most likely being associated with the presynaptic T bar identified by anti-Brp immunostaining.

We next tested whether Brp is required for the active zone–dependent localization of S6K. We expressed *UAS-Venus-S6K* in a *brp* mutant background lacking the synaptic Brp protein (Kittel et al., 2006). We find that S6K is no longer localized to active zones but is distributed broadly within individual boutons at or near the plasma membrane (Fig. 2 E). In addition, we quantified Brp staining intensity in *S6K* mutants and do not find a significant difference compared with wild type (wild type: 100%; *S6K*: 107.6%; $P > 0.05$), demonstrating that

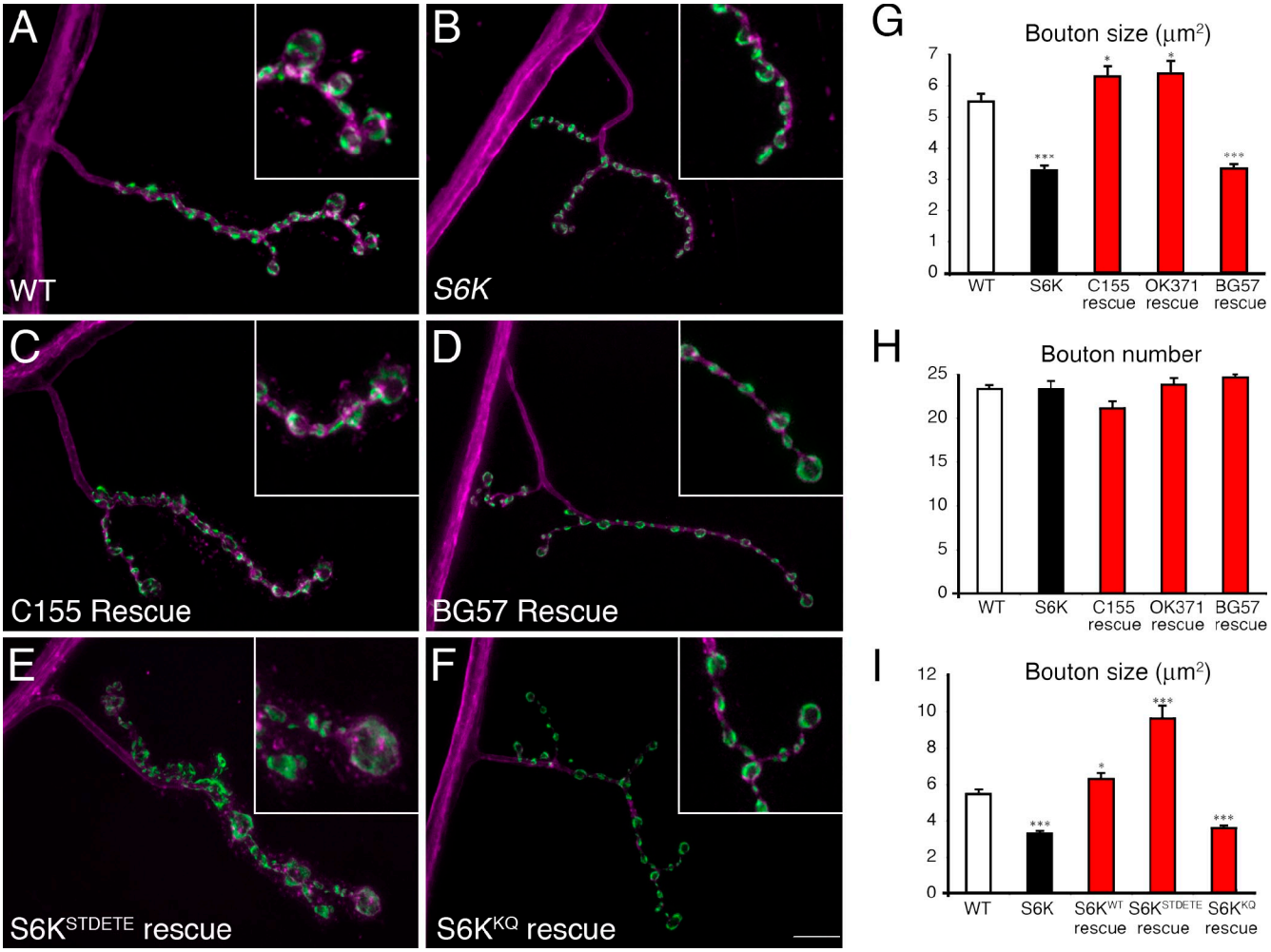

Figure 1. **Presynaptic S6K regulates bouton size without altering bouton number.** (A–F) Third instar NMJs on muscle 4 of segment A3 were visualized with the synaptic vesicle marker antisynapsin (green) and neuronal membrane marker HRP (magenta). Twofold magnifications from selected regions are shown in insets. Wild type (WT; A), *S6K^{l-1}/Df(3L)CH18* (B), *C155/+;UAS-S6K/+;S6K^{l-1}/Df(3L)CH18* (C), *UAS-S6K/+;S6K^{l-1},BG57/Df(3L)CH18* (D), *C155/+;UAS-S6K^{STDETE}/+;S6K^{l-1}/Df(3L)CH18* (E), and *C155/+;UAS-S6K^{KQ}/+;S6K^{l-1}/Df(3L)CH18* (F) are shown. (G–I) Quantification of bouton size (G and I) and bouton number (H). *n* > 10 for all genotypes. *, P < 0.05; ***, P < 0.0001. Error bars show SEM. Bar, 10 µm.

Brp localization to the active zone does not depend on S6K. We also asked whether expansion of active zone size would expand the size of the active zone–associated S6K puncta. It was recently demonstrated that active zones are dramatically enlarged in a *rab3* mutant background, and there is a corresponding enlargement of active zone–associated T bars that stain with Brp (Graf et al., 2009). When we overexpress *UAS-Venus-S6K* in a *rab3* mutant background, we find that the S6K remains colocalized with Brp. The S6K puncta are less dense, and the active zone–associated puncta of S6K appear to be enlarged in parallel with the Brp puncta, consistent with the *rab3* mutant phenotype (Fig. 2 F and not depicted; Graf et al., 2009). Together, these data confirm that S6K localizes to the presynaptic active zone and indicate that Brp is responsible for this localization, either directly or indirectly.

Next, we asked whether the active zone localization of S6K is functionally relevant. To do so, we examined bouton size in the *brp* mutant background in which S6K is mislocalized. We find that bouton size is decreased to levels that are not statistically significantly different from the S6K mutant alone (Fig. S3 A). Next, we asked whether overexpression of S6K would rescue bouton size in the *brp* mutant background. Overexpressed S6K does not localize to the active zones of the *brp* mutant (Fig. 2 E). Although there is a slight increase in bouton size compared with the *brp* mutant alone, this remains significantly smaller than wild-type controls. These data suggest that the localization of S6K to the presynaptic active zone is somehow essential for the normal function of S6K in determining bouton size. Interestingly, identical observations were made with respect to axon diameter. Axon diameter is smaller in the *brp* mutant, just as it is in the *S6K* mutant. Furthermore, overexpression of S6K fails to restore normal axon diameter in the *brp* mutant (Fig. S3 B). These data suggest that active zone–associated S6K might be a potent source of active S6K signaling that is important for regulating neuronal size, not just locally at the NMJ but perhaps throughout the cell.

S6K regulates active zones number and density

To quantify active zone number, we counted the number of Brp puncta per NMJ (Kittel et al., 2006; Wagh et al., 2006) as

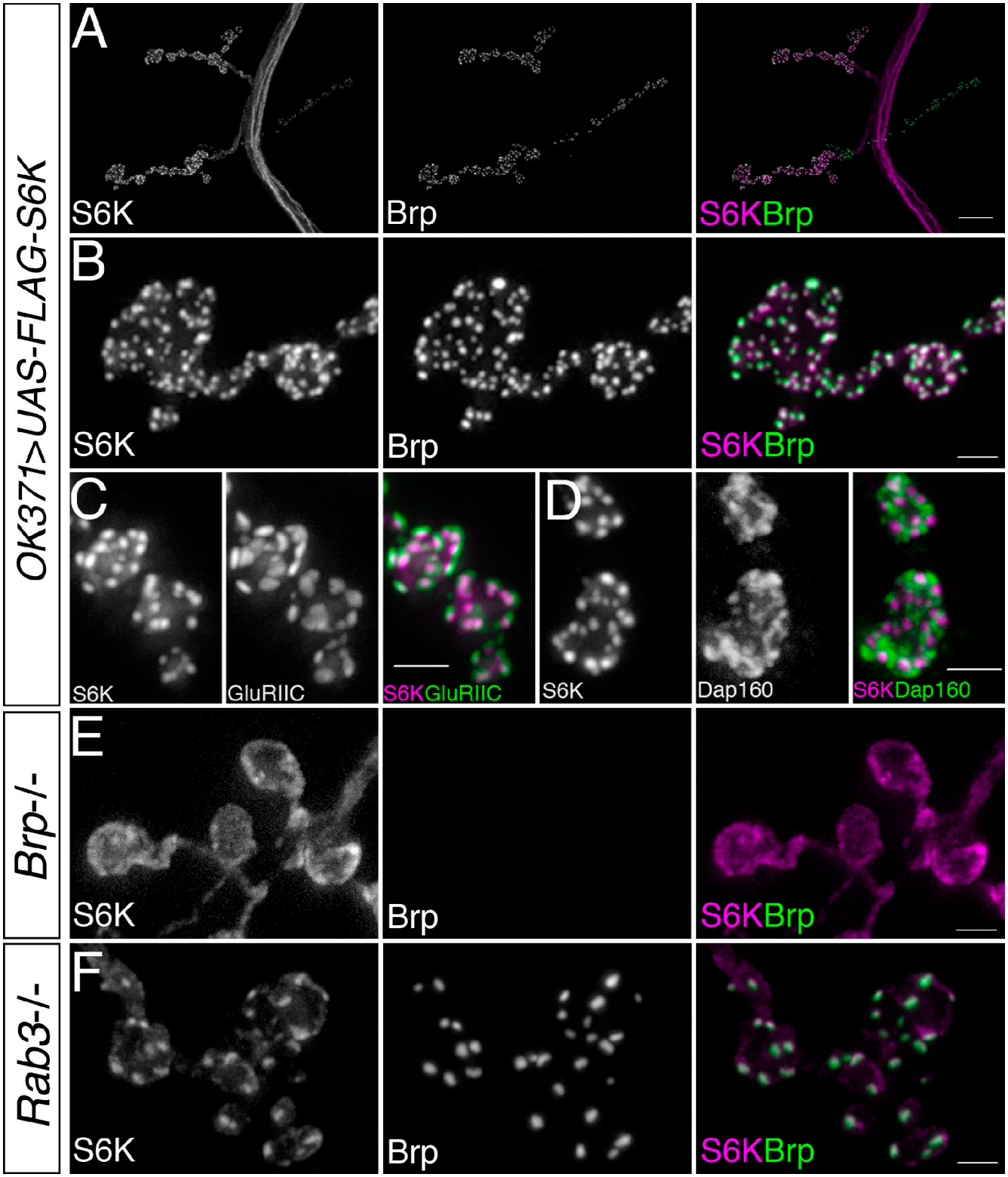

Figure 2. **S6K localizes to presynaptic active zones.** (A–D) Z-series projection of *OK371-Gal4/+;UAS-3×FLAG-S6K/+* NMJs at muscle 4. (A and B) Synapses are colabeled with anti-FLAG (S6K) and anti-Brp. (B) Higher magnification images from NMJ shown in A. (C) Synapses are colabeled with anti-FLAG (S6K) and anti-GluRIIC. (D) Synapses are colabeled with anti-FLAG (S6K) and anti-Dap160. (E) Z-series projection of *OK371-Gal4,Brp^{69}/Brp^{69}; UAS-Venus-S6K/+* synapses. Venus (S6K) and anti-Brp (absent in *brp* mutant) are shown. (F) Z-series projection of *C155/+;Rab3^{rup}/Rab3^{rup};UAS-Venus-S6K/+* synapses. Venus (S6K) and anti-Brp are shown. Bars: (A) 10 µm; (B–F) 2 µm.

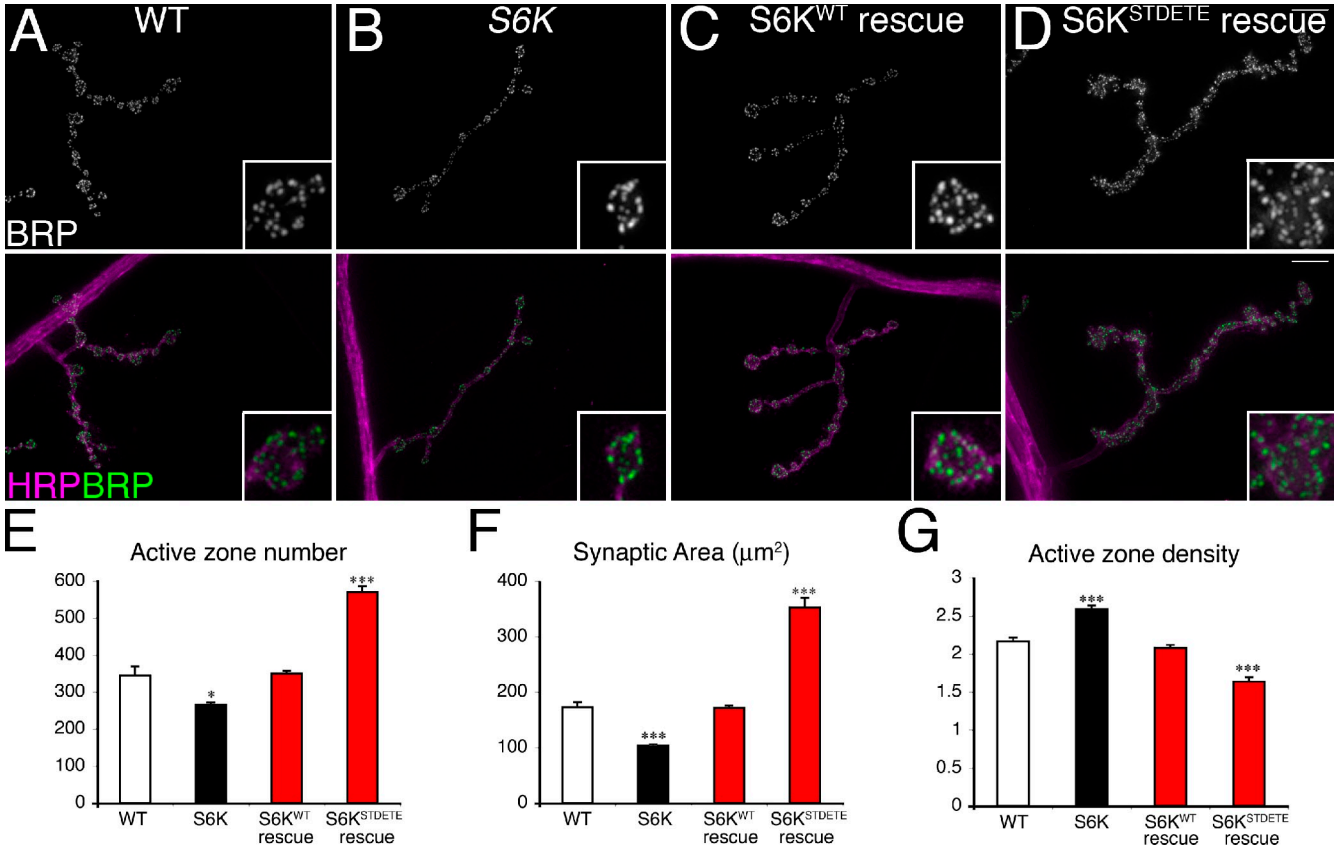

Figure 3. **S6K regulates active zone number and density.** (A–D) NMJs on muscle 4 of segment A3 are labeled with the active zone marker anti-Brp and neuronal membrane marker HRP. Insets represent higher magnification images of select synaptic boutons within each image. Wild type (WT; A), *S6K*$^{l\text{-}1}$/*Df(3L)CH18* (B), *C155/+;UAS-S6K/+;S6K*$^{l\text{-}1}$*/Df(3L)CH18* (C), and *C155/+;UAS-S6K*^{STDETE}*/+;S6K*$^{l\text{-}1}$*/Df(3L)CH18* (D) are shown. (E–G) Quantification of active zone number (E), synaptic area (F), and active zone density (G). $n > 10$ for all genotypes. *, $P < 0.05$; ***, $P < 0.0001$. Error bars show SEM. Bars, 10 μm.

previously performed (Pielage et al., 2006). *S6K* mutants have a significant decrease in active zone number compared with control (Fig. 3, B and E), and neuronal expression of *UAS-S6K* rescues this deficit in active zone number (Fig. 3, C and E). Surprisingly, neuronal expression of active *S6K* (*UAS-S6K*^{STDETE}) in the *S6K* mutant background is sufficient to increase total active zone number without altering bouton number (Fig. 3, D and E). We obtained similar results for the panneuronal driver *C155-Gal4* and the motoneuron-specific driver *OK371-Gal4* (unpublished data). Thus, S6K is necessary for the establishment of normal active zone numbers during development and sufficient to significantly increase active zone number. Because S6K localizes to the presynaptic active zone, we speculate that local S6K activity may be involved in controlling the number of active zones per synaptic bouton, though S6K is clearly not required for active zone formation per se because active zones do form in the *S6K* mutant.

Because S6K regulates bouton size and active zone number, we probed whether these two parameters always remain in register after the gain and loss of S6K activity. At the *Drosophila* NMJ, active zones are regularly spaced throughout the NMJ (Atwood et al., 1993). We find that the mean bouton area is decreased more than active zone number in the *S6K* mutant, causing an increase in active zone density (Fig. 3, E–G). Conversely, neuronal expression of active *S6K* (*UAS-S6K*^{STDETE}) in the *S6K* mutant background increases both bouton area and active zone number, but the parameters are not perfectly aligned, and active zone density is decreased compared with wild type (Fig. 3, F and G). Although these parameters are not in perfect register, it is remarkable that they are both influenced by S6K. Our data indicate that S6K, which resides at the active zone, has activity that could potentially couple changes in bouton size with active zone number, thereby coordinating structural and functional synaptic growth. It also remains formally possible that changes in active zone number are secondary to the changes in bouton size.

Finally, because S6K modulates synaptic bouton size, we asked whether S6K size control might extend to control the size of the individual synapses (defined as presynaptic Brp puncta opposed to a postsynaptic cluster of glutamate receptors). We examined *S6K* mutants and quantified the size of individual glutamate receptor fields, identified by antibodies against the glutamate receptor subunit GluRIIC (Marrus et al., 2004). We found no differences comparing control, *S6K* mutants, and neuronal rescue of *S6K* in terms of either the mean diameter of GluRIIC clusters (Fig. S4, A and B) or the distribution of GluRIIC cluster diameters (Fig. S4, A and B). Thus, the size of postsynaptic glutamate receptor clusters, reflecting the size of individual active zones, is not affected by presynaptic S6K activity.

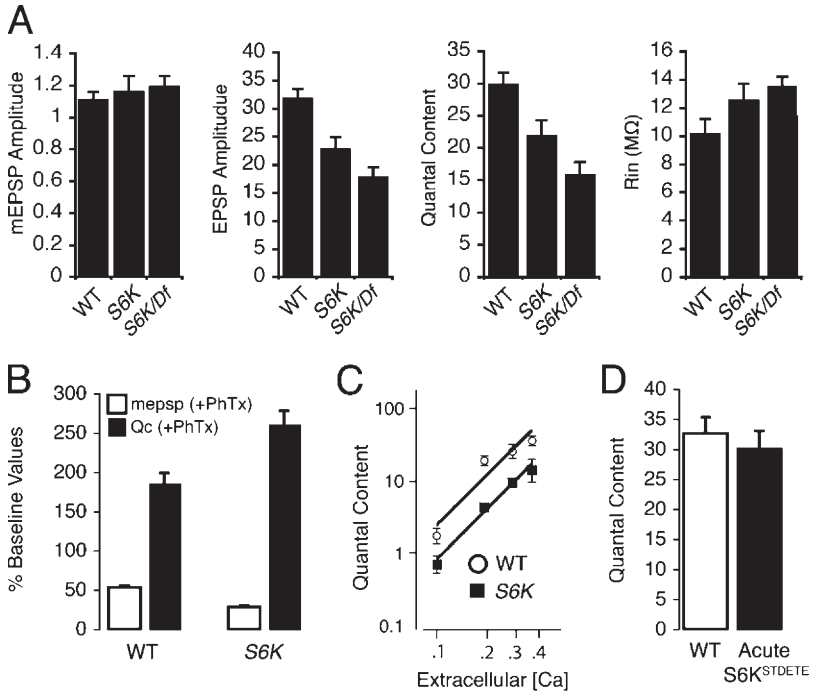

Figure 4. **Altered synaptic function at *S6K* mutant NMJ.** (A) Recordings are made from the NMJ at muscle 6, and data are shown for the mean mEPSP amplitude, mean EPSP amplitude, and mean quantal content (EPSP/mEPSP) and muscle input resistance (Rin). Genotypes in A include wild type (WT), *S6K*, and *S6K/Df* ($S6K^{l\text{-}1}/Df(3L)^{CH18}$). (B) Data are normalized to each genotype in the absence of PhTx as performed previously (Frank et al., 2006, 2009). Application of PhTx to the NMJ reduces mEPSP amplitudes and causes a significant increase in quantal content (Qc) compared with baseline (100%). (C) Extracellular calcium concentration is plotted against quantal content for the indicated genotypes. (D) Acute expression of $UAS\text{-}S6K^{STDETE}$ with *elav-Geneswitch* during the last 48 h of larval development is without effect on quantal content. Error bars show SEM.

S6K is necessary for normal synaptic function

Because S6K controls bouton size and active zone number, we asked whether S6K also controls the functional properties of the NMJ. First, we find that the mean amplitude of spontaneous miniature release events is unchanged in *S6K* mutants compared with wild type (Fig. 4 A). We also examined the abundance of the postsynaptic glutamate receptor subunits. Consistent with the lack of change in miniature excitatory postsynaptic potential (EPSP; mEPSP) amplitude, we did not detect a change in the abundance of GluRIIA or GluRIIC receptor subunits. However, we did find a minor, though statistically significant, increase in GluRIIB expression (Fig. S4). GluRIIB levels are restored toward wild-type values by presynaptic expression of *UAS-S6K* (wild type: 100 ± 3.53%; $S6K^{l\text{-}1}/df$: 160.35 ± 5.72%; *OK371/UAS-S6K;*$S6K^{l\text{-}1}/df$: 137.95 ± 3.53%). It does not appear, however, that the minor change in GluRIIB levels strongly influence the amplitude of the mEPSP. At this point, we also cannot rule out additional changes in one of the remaining glutamate receptor subunits (GluRIID and GluRIIE) that could counteract a change in GluRIIB.

Next, we examined evoked neurotransmitter release. Compared with wild type, *S6K* mutations have a significant decrease in mean EPSP amplitude (Fig. 4 A). There is also a correlated decrease in the quantal content observed in the *S6K* mutant background (Fig. 4 A). The smaller EPSP amplitude correlates well with the decrease in total active zone number, suggesting that this may be the cause of impaired muscle depolarization. Consistent with this conclusion, we find no change in paired pulse facilitation at the NMJ comparing wild-type and S6K mutants (unpublished data). There is no significant change in resting membrane potential (not depicted) or muscle input resistance (Fig. 4 A) that could account for the decrease in EPSP amplitude and quantal content. Finally, we observe a significant decrease in the rate of spontaneous miniature release events in the *S6K* mutations, also consistent with a decrease in active zone number (wild-type mEPSP frequency: 2.68 ± 0.16, $n = 12$; *S6K/Df* mEPSP frequency: 1.80 ± 0.16, $n = 12$; *S6K* mEPSP frequency: 1.80 ± 0.16, $n = 13$; $P < 0.001$ compared with wild type).

We performed two additional assays of synaptic function. We find that the defects in presynaptic release are consistent across a wide range of extracellular calcium concentrations, indicating that the calcium cooperativity of presynaptic release is unaltered in the *S6K* mutant background (Fig. 4 C). These data suggest that the calcium sensor for presynaptic release remains unaltered. We also tested whether S6K might have an acute function to alter presynaptic neurotransmitter release. To address this, we overexpressed active S6K using the gene-switch expression system, turning on $UAS\text{-}S6K^{STDETE}$ expression only during the final 48 h of larval development. However, the acute expression of this transgene had no effect on basal synaptic transmission (Fig. 4 D). These data suggest that the modulation of synaptic transmission is a developmental function of S6K.

Normal induction of homeostatic plasticity in S6K mutants

S6K has been implicated in learning-related synaptic plasticity in vertebrates (Cammalleri et al., 2003; Antion et al., 2008) and invertebrates (Khan et al., 2001; Weatherill et al., 2010). Therefore, we asked whether S6K is required for the homeostatic modulation of presynaptic release probability after inhibition of postsynaptic glutamate receptors with philanthotoxin (PhTx) at the *Drosophila* NMJ (Frank et al., 2006, 2009; Dickman and Davis, 2009; Bergquist et al., 2010; Marie et al., 2010). Application of PhTx significantly decreased mEPSP amplitudes in the *S6K* mutant background. However, we also observed a significant homeostatic increase in quantal content, indicating that

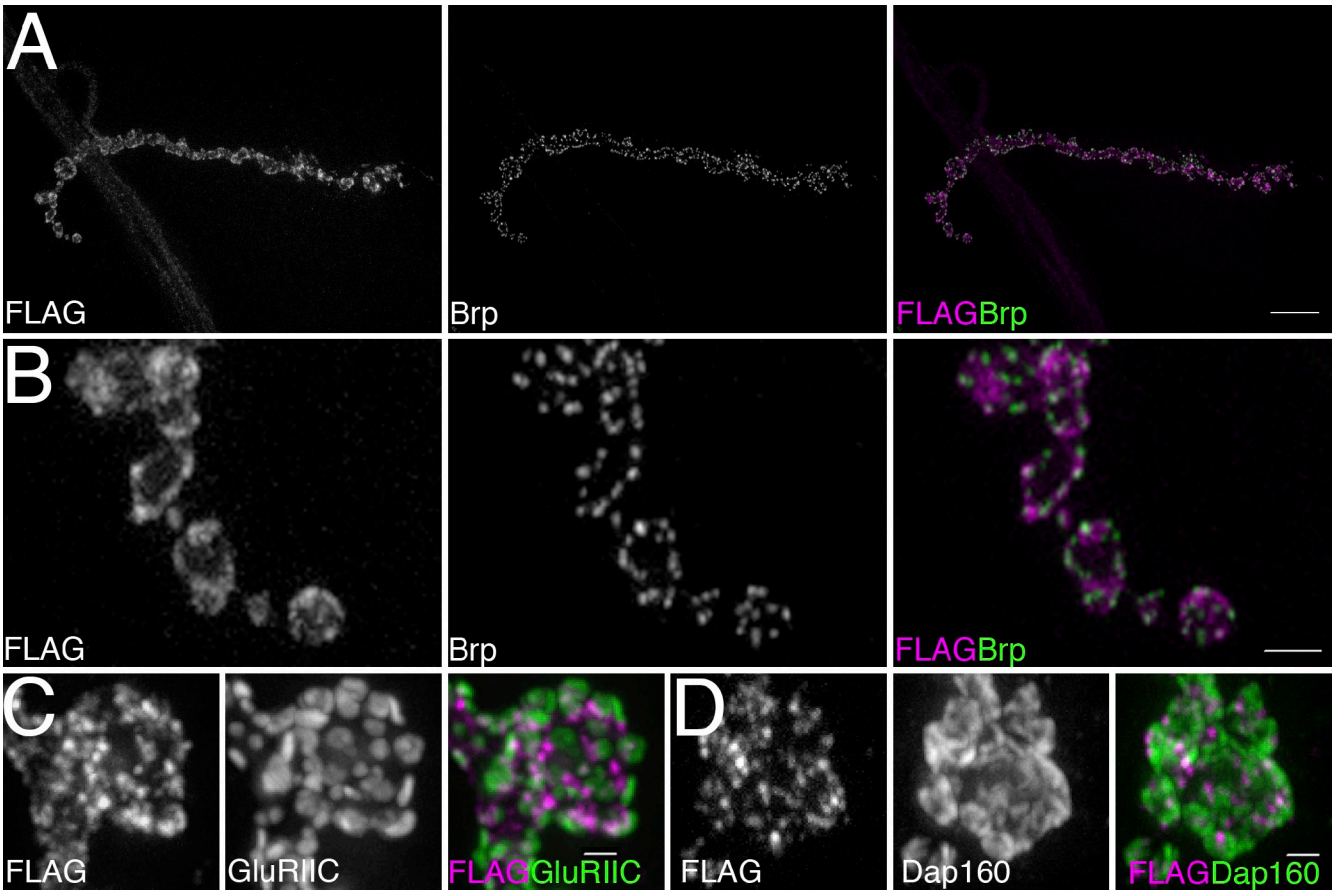

Figure 5. **PDK1 localizes to the *Drosophila* NMJs.** (A–D) Z-series projection of *OK371-Gal4/+;UAS-3×FLAG-PDK1/+* NMJs on muscle 4. (A) Synapses are colabeled with anti-FLAG (PDK1) and anti-Brp. (B) Higher magnification images of what is shown in A. (C) Synapses are colabeled with anti-FLAG (PDK1) and anti-GluRIIC. (D) Synapses are colabeled with anti-FLAG (PDK1) and anti-Dap160. Bars: (A) 10 µm; (B–D) 2 µm.

homeostatic plasticity is normal in the *S6K* mutant background (Fig. 4 B). We conclude that S6K is not required for the acute induction of homeostatic plasticity at the NMJ.

PDK1 localization at the NMJ

If S6K signaling functions locally at the active zone, one expects upstream kinase activity, necessary for S6K function, to be present at the NMJ as well. Therefore, we assessed the function of PDK1 (phosphoinositide-dependent protein kinase 1) at the NMJ. PDK1 is essential for activating several kinases, including PKA, PKC, and PKG as well as S6K (Mora et al., 2004). PDK1 has a pleckstrin homology domain, which binds to phosphatidylinositol (3,4,5)-triphosphate and phosphatidylinositol (3,4)-bisphosphate with high affinity, and likely regulates PDK1 subcellular localization. PDK1 appears to be constitutively active, and the activation of its downstream targets requires the conversion of its substrates into a conformation that can be accessed by PDK1 (Biondi, 2004).

We first asked whether *Drosophila* PDK1 traffics to the presynaptic nerve terminal at the *Drosophila* NMJ. We generated transgenic flies harboring *UAS-PDK1*, which includes a 3×FLAG tag at the N terminus of the transgene. When driven with the motoneuron-specific driver *OK371-Gal4*, the FLAG-PDK1 protein was detected in cell bodies, axons, and within presynaptic boutons. However, unlike S6K, the FLAG-PDK1 protein does not colocalize with the active zone marker Brp, the glutamate receptor subunit GluRIIC, or the periactive zone marker Dap160 (Fig. 5). We conclude that although presynaptic PDK1 traffics to the NMJ, it is not specifically localized within the active zone or periactive zone regions. When expressed in muscles with *BG57-Gal4*, FLAG-PDK1 was detected throughout muscles and, as with S6K, moderately enriched at the NMJ (Fig. S5).

PDK1 regulates bouton size and active zone number

In *Drosophila*, a previous study has shown that *PDK1*-null alleles die during the second instar, and hypomorphic alleles are viable, with decreased body size (Rintelen et al., 2001). Because these lines were unattainable, we generated new *PDK1* mutants through imprecise excision of *P{SUPor-P}KG01447*, which is inserted within an intron of the *PDK1* gene (Fig. S5). From 121 white-eyed lines, we obtained five lines that are first to second instar larval lethal and one line, $PDK1^{33}$, which can survive to the third instar stage and to the adult stage in reduced numbers. At larval stages, $PDK1^{33}$ resulted in smaller motoneuron cell bodies, similar to the findings in *S6K* mutants (Fig. S1). Adult flies homozygous for $PDK1^{33}$ displayed a severe reduction of body size when compared with wild type (Fig. S5). As a control, we also generated a precise excision line, $PDK1^{3}$, which

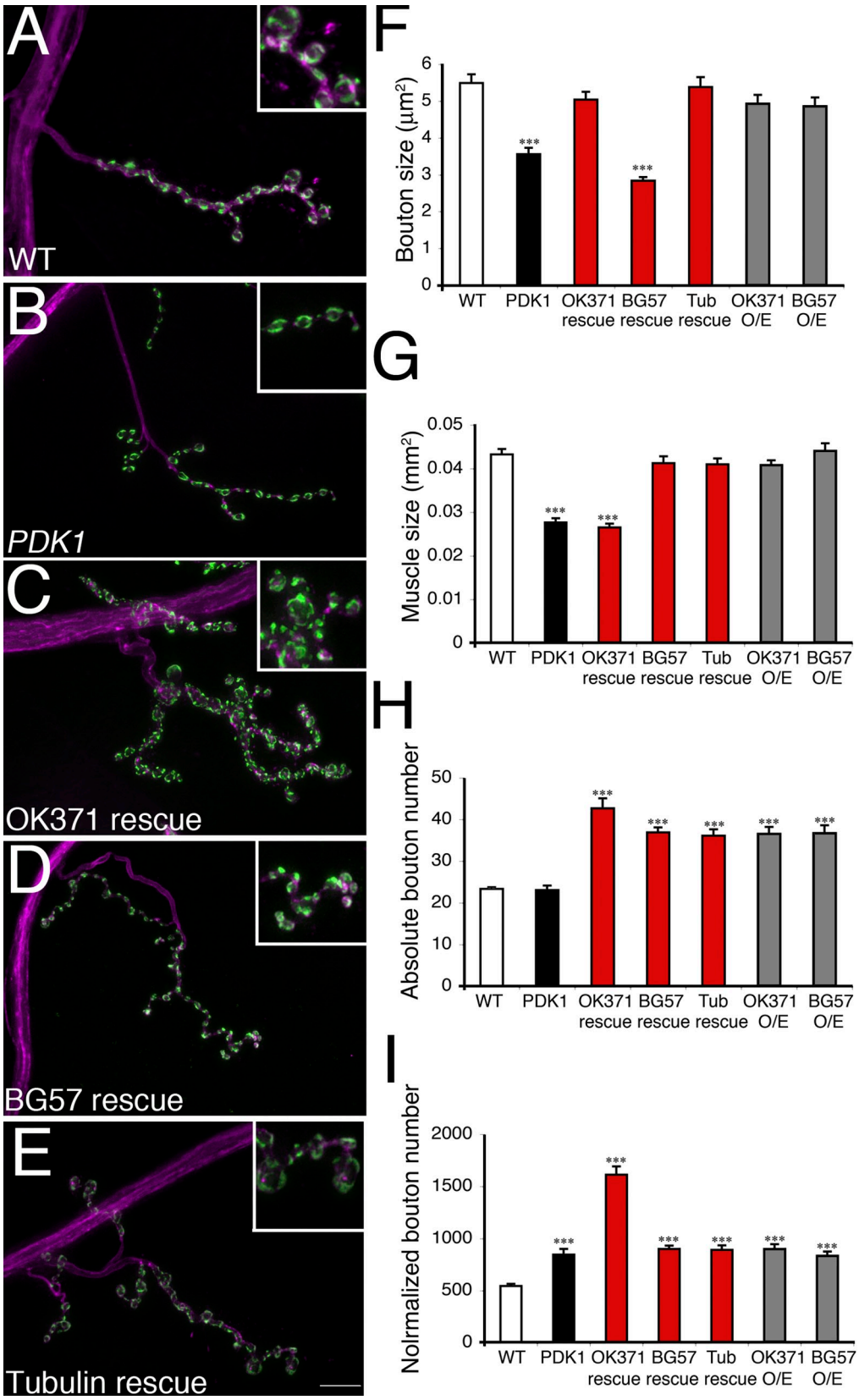

Figure 6. **PDK1 regulates bouton size, bouton number, and muscle size.** (A–E) Third-instar NMJs on muscle 4 of segment A3 are visualized with the synaptic vesicle marker antisynapsin (green) and neuronal membrane marker HRP (magenta). Twofold magnifications from selected regions are shown in insets. Wild type (WT; A), *PDK1^{33}/PDK1^{33}* (B), *OK371-Gal4/UAS-PDK1;PDK1^{33}/PDK1^{33}* (C), *UAS-PDK1/+;BG57-Gal4,PDK1^{33}/PDK1^{33}* (D), and *UAS-PDK1/+;Tubulin-Gal4,PDK1^{33}/PDK1^{33}* (E) are shown. (F–I) Quantification of bouton size (F), muscle size (G), absolute bouton number (H), and normalized bouton number (I). OK371 overexpression (O/E): *OK371-Gal4/UAS-PDK1*. BG57 overexpression: *UAS-PDK1/+;BG57-Gal4/+*. $n > 10$ for all genotypes. ***, $P < 0.0001$. Error bars show SEM. Bar, 10 µm.

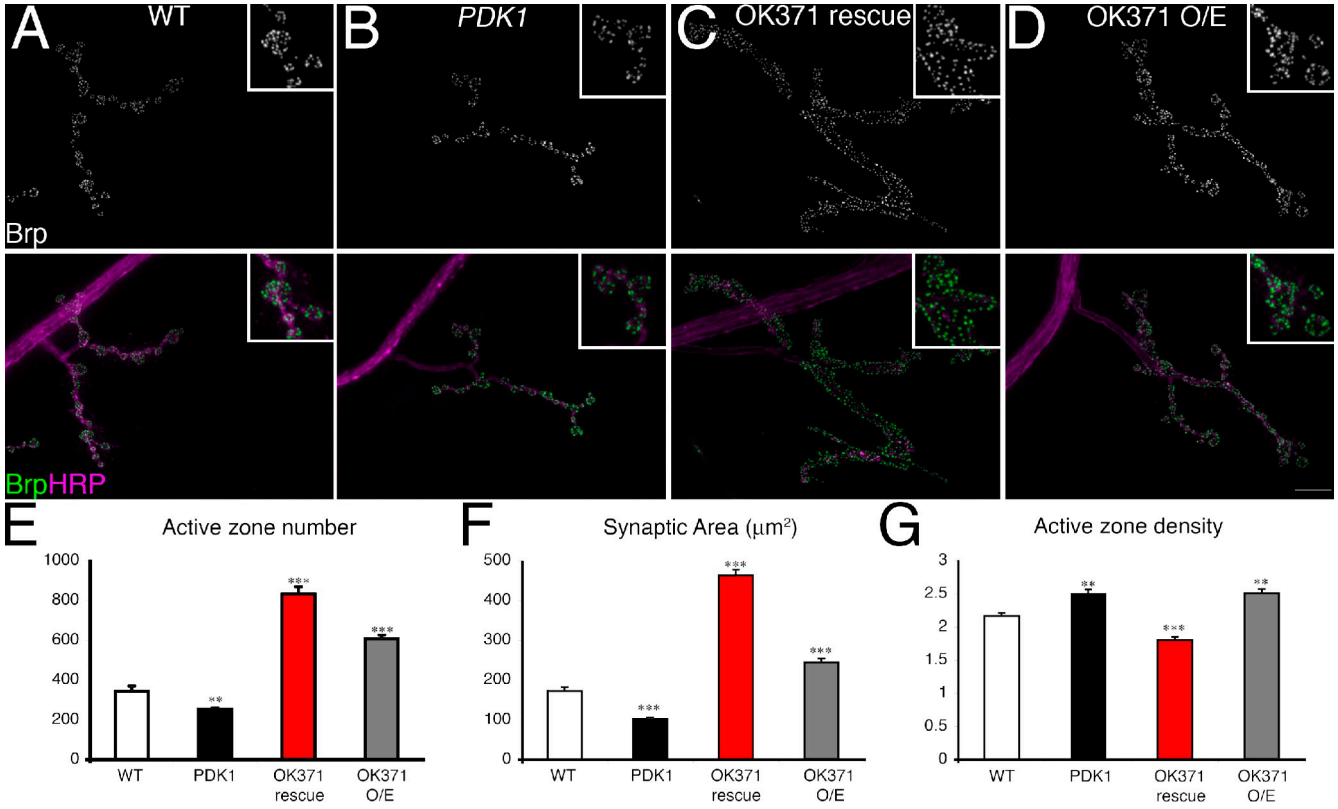

Figure 7. **PDK1 regulates active zone number and density.** (A–D) NMJs on muscle 4 of segment A3 are labeled with the active zone marker anti-Brp and neuronal membrane marker HRP. Insets represent higher magnification images of select synaptic boutons within each image. Wild type (WT; A), *PDK1*^{33}/*PDK1*^{33} (B), *OK371-Gal4/UAS-PDK1;PDK1*^{33}/*PDK1*^{33} (C), and *OK371-Gal4/UAS-PDK1* (D) are shown. (E–G) Quantification of active zone number (E), synaptic area (F), and active zone density (G). $n > 10$ for all genotypes. O/E, overexpression. **, $P < 0.01$; ***, $P < 0.0001$. Error bars show SEM. Bar, 10 μm.

is homozygous viable and has a normal body size. Our findings are consistent with previous findings that PDK1 regulates body size, most likely through the control of cell size.

The NMJs of *PDK1*^{33} mutants were phenotypically similar to those of *S6K* mutants. The *PDK1*^{33} mutants have normal bouton numbers and a significant 35% decrease of bouton size (Fig. 6, F and H). We also find that muscle fibers in *PDK1*^{33} mutants are significantly smaller than wild type, being 35% smaller than control (Fig. 6 G). This is in contrast with *S6K* mutants, which do not significantly affect muscle size. As a result of decreased muscle size, bouton number normalized to the muscle surface area of *PDK*^{33} was 55% higher than control (Fig. 6 I). These data suggest that PDK1 has growth-related functions both presynaptically and in muscle and that, in the absence of *PDK1*, the normally precise coupling between pre- and postsynaptic growth is impaired.

Next, we performed rescue experiments. Neuronal expression of *UAS-PDK1* with motoneuron-specific *OK371-Gal4* fully restored the defects in bouton size in *PDK1*^{33} but did not restore the defects in muscle size (Fig. 6, F and G). In contrast, muscle expression of *UAS-PDK1* with *BG57-Gal4* fully restored the defects in muscle size but failed to rescue the defects in bouton size (Fig. 6, F and G). From these data, we can conclude that PDK1 has a specific function in the motoneuron for the control of bouton size, most likely acting upstream of S6K.

Surprisingly, although loss of PDK1 does not alter the absolute number of boutons at the third instar NMJ, overexpression of *UAS-PDK1* is sufficient to increase bouton number (Fig. 6, H and I). These data suggest that PDK1 can modulate bouton size and can also drive the elaboration of new synaptic boutons through an S6K-independent mechanism. Interestingly, this is also true for postsynaptic overexpression of PDK1. This gain-of-function phenotype suggests that postsynaptic PDK1 can promote trans-synaptic signaling that influences total bouton number. However, because PDK1 loss-of-function mutations do not alter bouton number, PDK1 is not necessary, presynaptically or postsynaptically, for the elaboration of bouton number.

Next, we examined the number of active zones in *PDK1* mutants. Similar to the phenotype of *S6K* mutants, *PDK1* mutants displayed a reduction of the number of active zones per NMJ, a decrease in synaptic area, and an increase of active zone density compared with control (Fig. 7). Because total bouton number remained unchanged in the *PDK1* mutant, the change in total active zone number is correlated with a change in bouton size, as observed for *S6K*. Neuronal rescue of *PDK1* led to an increase in the number of active zones, an increase of synaptic area, and a decrease of active zone density compared with wild type (Fig. 7). Neuronal overexpression of PDK1 in a wild-type background caused an increase of the number of active zones, an increase of synaptic area, and a small increase of active zone

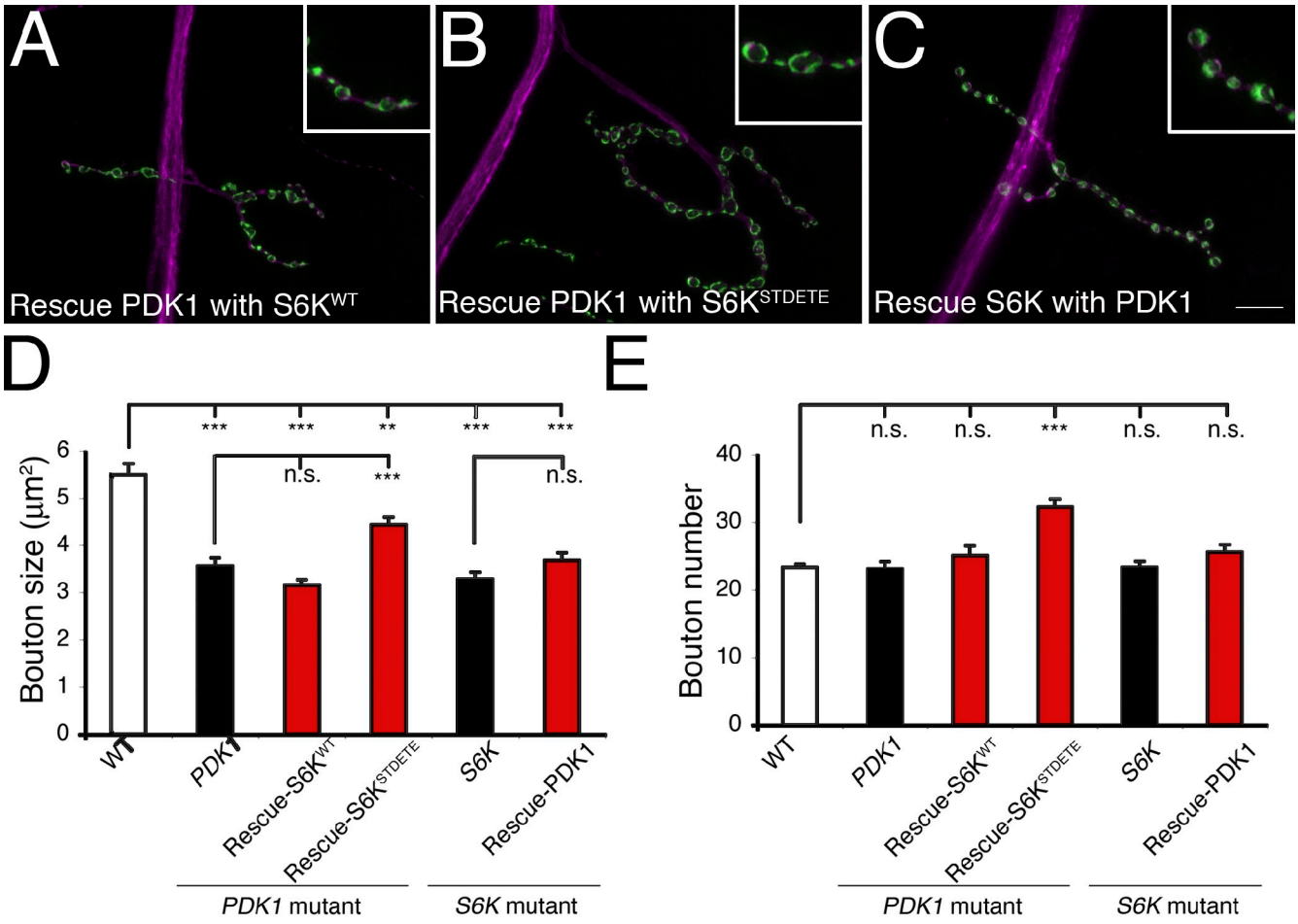

Figure 8. **Neuronal overexpression of active S6K is able to rescue bouton size defects in PDK1 mutants.** (A–C) Third instar NMJs on muscle 4 of segment A3 are visualized with the synaptic vesicle marker antisynapsin and neuronal membrane marker HRP. Twofold magnifications from selected regions are shown in insets. *OK371-Gal4/UAS-S6K;PDK1^{33}/PDK1^{33}* (A), *OK371-Gal4/UAS-S6K^{STDETE};PDK1^{33}/PDK1^{33}* (B), and *OK371-Gal4/UAS-PDK1;S6K^{l-1}/Df(3L)CH18* (C) are shown. (D and E) Quantification of bouton size (D) and bouton number (E). $n > 10$ for all genotypes. **, $P < 0.01$; ***, $P < 0.0001$. Error bars show SEM. Bar, 10 µm.

density (Fig. 7). Thus, similar to S6K, PDK1 is sufficient to alter the number and density of active zones within the NMJ. It is unclear why expression of PDK1 in the PDK1 mutant is more effective than expression in a wild-type background, though it could have something to do with the timing of early PDK1 expression that might differ between wild-type and mutant backgrounds.

Genetic interactions between S6K and PDK1

We next performed genetic epistasis experiments to test the functional relationship between S6K and PDK1 during NMJ development. It is well established that PDK1 is an important upstream regulator of S6K, both in vitro and in vivo (Dennis et al., 1998; Radimerski et al., 2002). S6K activation requires multiple interdependent phosphorylation events in its autoinhibitory domain, the linker region, and the catalytic domain. Many of these residues are highly conserved in *Drosophila* S6K (Barcelo and Stewart, 2002). Substitution of conserved residues in the autoinhibitory domain and the linker region to acidic residues enhances kinase activity in the wing-bending assay (Barcelo and Stewart, 2002). Furthermore, a genetic study in flies shows that *Drosophila* S6K activation depends on PDK1 (Radimerski et al., 2002).

To test whether PDK1 acts via S6K to control bouton size, we first attempted to rescue *PDK1* mutants with a neuronally expressed *S6K* transgene. We tested both *UAS-S6K* and the hyperactive *UAS-S6K^{STDETE}*. The *UAS-S6K* transgene needs to be phosphorylated at both the autoinhibitory domain and the linker region before it can be phosphorylated by PDK1 and become fully active (Dennis et al., 1998). The *UAS-S6K^{STDETE}* transgene, with phosphomimic residues in the autoinhibitory domain and the linker region, is partially active and only needs PDK1-mediated phosphorylation at the activation loop to become fully active. We reason that the remaining PDK1 activity in the hypomorphic *PDK1^{33}* may be sufficient to achieve some activation of *S6K^{STDETE}*, and *S6K^{STDETE}* might, therefore, be more effective than wild-type S6K at achieving rescue. Indeed, *UAS-S6K^{STDETE}* partially rescues the bouton size defect of *PDK1* mutants, whereas *UAS-S6K* fails to rescue (Fig. 8). The bouton size of *UAS-S6K^{STDETE}* expression in *PDK1* was significantly increased from the level of *PDK1* mutants alone, although not fully back to the control level (Fig. 8 D). It is worth noting that

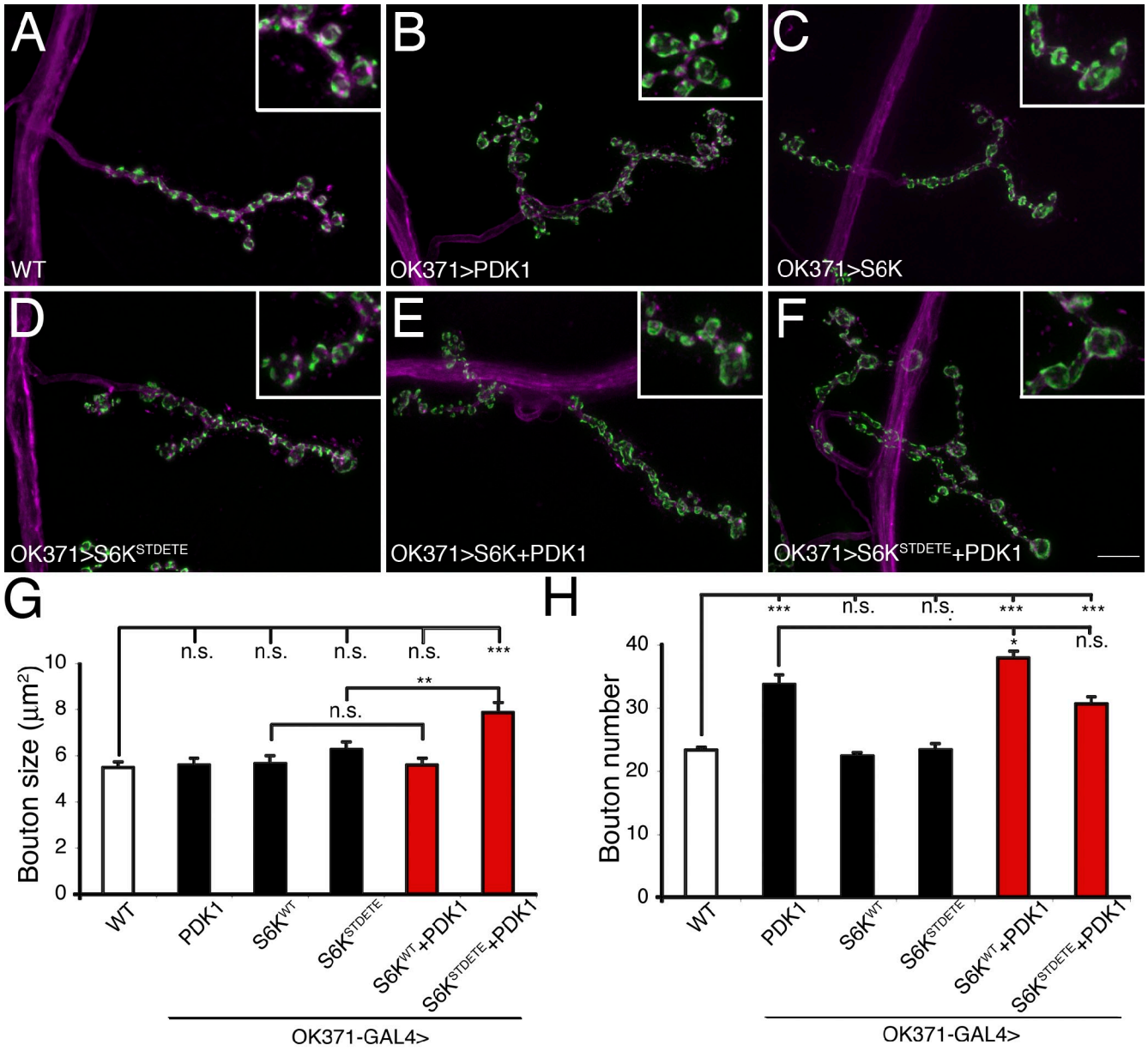

Figure 9. **Simultaneous overexpression of S6K and PDK1 increases bouton size and bouton number.** (A–F) Third instar NMJs on muscle 4 of segment A3 are visualized with the synaptic vesicle marker antisynapsin and neuronal membrane marker HRP. Twofold magnifications from selected regions are shown in insets. Wild type (WT; A), *OK371-Gal4/+;UAS-PDK1/+* (B), *OK371-Gal4/UAS-S6K* (C), *OK371-Gal4/UAS-S6K*^{STDETE} (D), *OK371-Gal4/UAS-S6K;UAS-PDK1/+* (E), and *OK371-Gal4/UAS- S6K*^{STDETE}*;UAS-PDK1/+* (F) are shown. (G and H) Quantification of bouton size (G) and bouton number (H). $n > 10$ for all genotypes. *, $P < 0.05$; **, $P < 0.01$; ***, $P < 0.0001$. Error bars show SEM. Bar, 10 µm.

overexpression of *UAS-S6K*^{STDETE} increases bouton number in the PDK1 mutant background (Fig. 8 E). Under this condition, it appears that active S6K might also be sufficient to influence bouton number as well as size and is able to do so independent of PDK1. As a control, overexpression of *UAS-S6K* or *UAS-S6K*^{STDETE} alone doesn't influence bouton size or bouton number (Fig. 9, G and H). We also attempted to rescue *S6K* mutants with neuronally expressed PDK1. If PDK1 is upstream of S6K, increasing PDK1 expression will not be able to compensate for the loss of S6K. Indeed PDK1 failed to rescue the bouton size defects of *S6K* mutants (Fig. 8 D) and did not induce a change in bouton number as predicted (Fig. 8 E). Collectively, these findings suggest that PDK1 regulates bouton size through activation of S6K.

Next, we were interested in whether overexpression of PDK1 and/or S6K can enhance synaptic growth. Having shown that overexpression of PDK1 can increase bouton number without affecting bouton size, we investigated whether S6K overexpression has any effect and whether simultaneous overexpression of both S6K and PDK1 can have a synergistic effect on synaptic growth. Using the motoneuron-specific driver *OK371-Gal4*, we find that overexpression of either *UAS-S6K* or hyperactive *UAS-S6K*^{STDETE} alone failed to affect bouton size or bouton number (Fig. 9; note that overexpression

on a wild-type background is different than transgene expression in the null background as in Fig. 8, and see Fig. 1 for additional data regarding expression of *UAS-S6K* using additional neuron-specific drivers). Next, we simultaneously overexpressed *UAS-PDK1* with either *UAS-S6K* or *UAS-S6K*^{STDETE}. Because PDK1 is constitutively active, whereas S6K needs to be phosphorylated at the autoinhibitory domain and the linker region before it can be activated by PDK1, we reason that increasing the levels of PDK1 will be able to activate ectopically expressed S6K^{STDETE} but may not activate ectopically expressed wild-type S6K. We found that cooverexpression of *UAS-S6K* with *UAS-PDK1* was similar to *UAS-PDK1* overexpression alone, causing increased bouton number and normal bouton size (Fig. 9, E–H). In contrast, cooverexpression of *UAS-PDK1* and *UAS-S6K*^{STDETE} led to a 43% increase of bouton size and a 31% increase of bouton number (Fig. 9, F–H). These results suggest that PDK1 overexpression, not S6K overexpression, is able to increase bouton number, whereas PDK1 and S6K together, most likely through hyperactivation of S6K, can enhance bouton size. These results support our model that, at the *Drosophila* NMJ, PDK1 regulates bouton size through S6K, whereas PDK1 can also influence total bouton number through another pathway, independent of S6K.

Discussion

Specification of neuronal dimension

The formation of complex neural circuitry is largely determined by the sequential processes of axon guidance, target recognition, and the activity-dependent refinement of synaptic connectivity. However, the dimensions of individual neuronal compartments, including the length and diameter of dendrites, axons, and presynaptic boutons are also reproducibly specified for each cell type, and these parameters strongly influence neuronal function. It was previously established that PDK1 and S6K control cell size (Montagne et al., 1999; Rintelen et al., 2001), but it has remained unclear how these potent signaling molecules influence synaptic growth. Here, we provide evidence that signaling through PDK1 and S6K is specifically required to control synaptic bouton size without strongly influencing the proliferation of bouton number or the length of the nerve terminal. Many genes have been identified that perturb synapse morphology at the *Drosophila* NMJ when mutated (Roos et al., 2000; Wan et al., 2000; Kaufmann et al., 2002; Marqués et al., 2002; Packard et al., 2002; Sweeney and Davis, 2002; Sherwood et al., 2004; Miech et al., 2008; Pielage et al., 2008; Shen and Ganetzky, 2009). In most cases, however, the gross morphology of the synapse is perturbed, indicating that the cellular mechanics of nerve terminal extension are altered. In contrast, signaling via PDK1 and S6K primarily control the dimensions of individual synaptic boutons without otherwise altering the appearance of the presynaptic terminal.

How are changes in compartment dimensions (cell diameter, axon diameter, and bouton diameter) mechanistically executed downstream of PDK1 and S6K? It is particularly interesting that both PDK1 and S6K are distributed throughout the cell, being present in axons, presynaptic terminals, and in the case of S6K, at the active zone. This distribution suggests that PDK1 and S6K could exert local effects that contribute to the specification of cell shape. Indeed, there is a correlation between impaired S6K localization at the active zone in the *brp* mutant and decreased bouton size as well as decreased axon size. Future experiments will be necessary to determine whether the changes in compartment size are a direct consequence of S6K mislocalization or whether size is influenced by altered synaptic transmission in the *brp* mutant. It is interesting to speculate about the cell biological processes that might function downstream of S6K to influence cellular dimensions. A previous study has provided evidence that the submembranous skeleton composed of spectrin and ankyrin provides structural integrity and modulates the shape of axons and presynaptic terminals, in part through organization of the underlying microtubule cytoskeleton (Pielage et al., 2008). However, a connection between PDK1, S6K, and the submembranous spectrin/ankyrin skeleton remains to be identified. In other systems, S6K has been shown to interact with spinophillin/neurabin, which is an F-actin– and protein phosphatase 1–binding protein linked to the control of dendritic spine size in vertebrates and active zone integrity in *Caenorhabditis elegans* (Burnett et al., 1998; Oliver et al., 2002; Ryan et al., 2005; Sieburth et al., 2005; Terry-Lorenzo et al., 2005). A link between S6K and neurabin/spinophillin could provide a mechanism to link local nutrient detection to the modulation of the neuronal cytoskeleton and cell shape.

Control of active zone number

It remains unknown how active zone number is specified for a given cell type. The neuromuscular synapse, the Calyx of Held, and other large, powerful synapses harbor a robust and reproducibly large number of active zones. In contrast, other neuronal cell types make synaptic connections composed of fewer active zones, many forming a single release site within a synaptic bouton. Genes have been identified that negatively regulate active zone assembly (Johnson et al., 2009; Patel and Shen, 2009). Other genes have been identified that are necessary for correct placement of active zones (Shen and Bargmann, 2003; Colón-Ramos et al., 2007), active zone assembly (Dai et al., 2006; Fouquet et al., 2009), and active zone dimensions (Graf et al., 2009). In contrast, the specification of total active zone number has remained less well defined. Target-derived growth factors clearly influence the growth and development of the presynaptic nerve terminal and have been shown to influence total active zone number (Nguyen et al., 1998; McCabe et al., 2003). These signaling systems will activate downstream intracellular signaling cascades, such as MAPK signaling, recently implicated in the specification of active zone number at the *Drosophila* NMJ (Wairkar et al., 2009). However, it also seems likely that the control of active zone number during development will be more complex than simple specification based upon the quantity of a target-derived trophic signal. We speculate that there will exist cell type–specific programs that interface with growth factor signaling to determine characteristic active zone densities. Cellular metabolic signaling might be one such cell type–specific parameter, including the actions of S6K and PDK1.

It is particularly remarkable that presynaptic overexpression of S6K and PDK1 are sufficient to increase active zone number at the NMJ. These data indicate that synapse assembly during

neuromuscular development is a process that can be driven by signaling that originates within the motoneuron. We speculate that the localization of S6K at the active zone may be critical in this regard. In some respects, it seems counterintuitive that a signaling system coupled to the metabolism of the motoneuron (PDK1-S6K) would be able to determine active zone number and, therefore, the level of postsynaptic excitation. Therefore, in keeping with well-established trophic mechanisms (Purves and Lichtman, 1978), we predict that S6K and PDK1 normally function downstream of muscle-derived factors, including nutrients and growth factors, that couple the needs of the muscle to the insertion of active zones by the motoneuron.

Presynaptic protein translation

There is increasing evidence that local protein synthesis plays a prominent role within postsynaptic dendrites (Akins et al., 2009). In contrast, the evidence for presynaptic protein translation is less abundant, including an apparent absence of polyribosomes within axons and nerve terminals (Akins et al., 2009). The most convincing evidence for local presynaptic protein translation is observed in *Aplysia*, in which serotonin-dependent long-term facilitation can be induced in synaptic compartments separated from the soma. Interestingly, two recent studies implicate S6K in presynaptic, translation-dependent long-term facilitation in *Aplysia* (Khan et al., 2001; Weatherill et al., 2010). The localization of S6K to the presynaptic active zone, where additional RNA-interacting signaling molecules have recently been identified (Johnson et al., 2009), is intriguing. In *Drosophila*, the translational repressors nanos and pumillio have been implicated in the regulation of neuromuscular growth (Menon et al., 2004, 2009), membrane excitability (Mee et al., 2004), and postsynaptic glutamate receptor abundance (Menon et al., 2004). Nanos is present presynaptically, and recent data demonstrate that loss of nanos leads to an increase in total bouton number and an increase in the total active zone number (Menon et al., 2009). In a separate study, the IGF-II RNA-binding protein (Imp-GFP) was observed to traffic to the presynaptic terminal, and loss of *Imp* caused a decrease in bouton number (Boylan et al., 2008). Although none of these data provide direct evidence for local presynaptic protein translation being important for presynaptic development or function, there is an accumulation of data suggesting that this may be a realistic possibility. Perhaps local protein translation, downstream of nutrient and growth factor signaling, could help independently shape the dimensions of each neuronal compartment (soma, axon, dendrite, and nerve terminal) and, thereby, fine tune the input–output properties of neurons during development. In this regard, it is particularly interesting that the synaptic localization of S6K by Brp seems to be important for size regulation at the synapse and perhaps throughout the cell.

Materials and methods

Fly stocks

The following strains were used in this study: *w1118* (wild type), *C155-Gal4* (Lin and Goodman, 1994), *OK371-Gal4*, *BG57-Gal4* (Budnik et al., 1996), and *Tubulin-Gal4*. $S6K^{l\text{-}1}$ was a gift from G. Thomas (Friedrich Miescher Institute for Biomedical Research, Basel, Switzerland; Montagne et al., 1999). The following lines were obtained from the Bloomington Stock Center: *Df(3L)CH18* (deficiency for S6K), $UAS\text{-}S6K^{KQ}$, $UAS\text{-}S6K^{STDETE}$, and *P{SUPor-P}KG01447*. Excision lines of PDK1 were generated by the excision of the *P* element line *P{SUPor-P}KG01447* using the Δ2–3 transposase. Putative excisions were balanced over *TM6b* and screened for lethality. Homozygous lethal lines were subsequently screened with PCR using primers 5′-TCTTTTCGCGAATTCCAGTT-3′ and 5′-GCCGCTTCTCGCATACTTTA-3′. This set of primers gave rise to a 763-bp band in wild type and a 1.3-kb band in the line $PDK1^{33}$. Sequencing of PCR products revealed that ∼600 bp of the *P* element sequence were left at the insertion site in the $PDK1^{33}$ line.

Transgenic constructs

To generate the UAS-S6K construct, the ORF of *S6K* was amplified from a cDNA library using PCR primers 5′-CACCATGGCGGACGTGAGCGAT-3′ and 5′-TTAGACCATCGGCAGACCCTGC-3′. The PCR product was cloned into the pENTR/D-TOPO vector (Invitrogen). To generate the *UAS-PDK1* construct, the ORF of *PDK1* was amplified from the cDNA clone LD22131 (from the Drosophila Genomics Resource Center) using PCR primers 5′-CACCATGCCGGCTATGGCCAAG-3′ and 5′-TTACTTAGACGCCGTCTTCTTGC-3′. The PCR product was cloned into the pENTR/D-TOPO vector. For both constructs, positive clones were recombined with the destination vector pTFW and pTVW (Drosophila Gateway Vector Collection from the Murphy laboratory), which contains a triple FLAG tag at the N terminus and a Venus tag at the N terminus, respectively. Standard procedures were used to transform the constructs into flies and to map the insertion chromosomes.

Immunohistochemistry

Wandering third instar larvae were dissected in HL3 saline and fixed with Bouin's fixative (Sigma-Aldrich) for 1 min at room temperature or with 4% paraformaldehyde for 10 min at room temperature. Primary antibodies were used at the following dilutions: antisynapsin (3C11) at 1:10, anti-Brp (nc82) at 1:100, and anti-GluRIIA (8B4D2) at 1:10 (all obtained from Developmental Hybridoma Bank); anti-FLAG (M2) was obtained from Sigma-Aldrich and used at 1:1,000; rabbit anti-GluRIIC and rabbit anti-GluRIIB were gifts from A. DiAntonio (Washington University, St. Louis, MO) and used at 1:1,000 and 1:2,500, respectively; rabbit anti-Dap160 (Marie et al., 2004) was used at 1:1,000. Secondary antibodies were Alexa Fluor 488 or Alexa Fluor 555 conjugated (Invitrogen) and used at 1:200–1:600. Cy3- and Cy5-conjugated HRP (Jackson ImmunoResearch Laboratories, Inc.) were used at 1:50–1:100. To colabel Brp and FLAG, an Alexa Fluor 488 mouse IgG1 labeling kit and Alexa Fluor 555 mouse IgG1 labeling kit (Zenon; Invitrogen) were used according to manufacturer's protocols.

Imaging and analysis

Images of NMJs were captured with a microscope (Axioskop 2000M; Carl Zeiss) and a cooled charged-coupled device camera (CoolSNAP HQ; Roper Scientific) with a Plan Apochromat 100× oil immersion lens (NA = 1.40; Carl Zeiss). All images were taken at room temperature using imaging oil (Immersol; Carl Zeiss). Image acquisition and analysis were performed in SlideBook software (Intelligent Imaging Innovation). A stack of images was acquired for each synapse, and the deconvolved projection image was used for analysis. Using the SlideBook software, stacks were deconvolved with the nearest neighbor algorithm and, subsequently, combined into a single projection image. Analysis of bouton size and bouton number was performed with the type Ib boutons on muscle 4 at segment A3 in third instar larvae. Bouton number was then determined by counting the total number of type Ib boutons on muscle 4 at segment A3. Muscle size was quantified by measuring surface area of muscle 4 at segment A3 in third instar larvae. Normalized bouton number was determined by dividing bouton number by muscle size. Active zone numbers were determined by counting the number of Brp-positive puncta in type Ib boutons on muscle 4 at segment A3. Synaptic area was determined by measuring the area of continuous HRP staining from the first synaptic bouton to the terminal boutons. Active zone density was determined by dividing the number of active zones by synaptic area. For quantification of glutamate receptor fluorescence intensity, the synaptic region of interest was defined by first imaging costained anti-HRP. Glutamate receptor fluorescence intensity was quantified by measuring the mean glutamate receptor intensity across this region of interest in a 2D confocal projection image as performed previously (Albin and Davis, 2004). We defined the synaptic area as delimited by HRP immunoreactivity and then quantified glutamate receptor staining intensity within this synaptic area using SlideBook software semiautomated routines as described previously (Albin and Davis, 2004). Images of the ventral nerve cord were captured with a confocal microscope (SP2; Leica), and image analysis was performed with ImageJ (National Institutes of Health).

Statistical analysis was performed with one-way analysis of variance. All data were shown as means ± SEM.

Electrophysiology

Third instar larvae were selected and dissected according to previously published techniques (Pielage et al., 2008). In brief, larvae were selected at the wall climbing state of late third larval instar. Animals were filleted with a dorsal incision, and the gut was removed along with the central nervous system using fine scissors. The fillet was held open at the anterior and posterior extremes as well as at the four corners using pressure pins on a glass slide, held in place by magnetic strips adjacent to the glass slide. Whole-muscle recordings were performed on muscle 6 in abdominal segment A3 using sharp microelectrodes (12–16 MΩ). Recordings were selected for analysis only if resting membrane potentials were more hyperpolarized than 60 mV and if input resistances were >5 MΩ. The mean spontaneous mEPSP amplitude was quantified by measuring the amplitude of ∼100–200 individual spontaneous release events per NMJ. The mean per-NMJ mEPSP amplitudes were then averaged for each genotype. Measurement of mEPSP amplitudes was semiautomated (Synaptosoft, Inc.). The mean super threshold–evoked EPSP amplitude was calculated for each NMJ, ensuring that both motor axons innervating muscle 6 in segment A3 were recruited. Quantal content was calculated as the mean EPSP amplitude divided by the mean mEPSP amplitude. Quantal content was determined for each NMJ and then averaged across NMJ to generate the mean quantal content for each genotype. Data for steady-state synaptic transmission were acquired in HL3 saline (0.4 mM Ca^{2+} and 20 mM Mg^{2+}). Data were collected using an amplifier (Axoclamp 2B; Axon Instruments), an analogue to digital board (Digidata 1200B; Axon Instruments), a pulse stimulator (Master-8; A.M.P.I.), and pCLAMP software (Axon Instruments). Data were analyzed off line using Mini Analysis software (Synaptosoft, Inc.).

Online supplemental material

Fig. S1 shows data demonstrating that loss of S6K and PDK1 results in smaller motoneuron cell size. Fig. S2 provides data for localization of postsynaptically expressed S6K and presynaptically expressed Venus-tagged S6K. Fig. S3 shows data demonstrating that loss of Brp results in smaller boutons and axons. Fig. S4 provides analysis of postsynaptic glutamate receptor clusters. Fig. S5 shows the PDK1 genomic region and evidence that postsynaptically expressed PDK1 localizes diffusely in the muscle as well as the effect of loss of PDK1 on body size for *Drosophila*. Online supplemental material is available at http://www.jcb.org/cgi/content/full/jcb.201101042/DC1.

This work was supported by National Institutes of Health grants NS047342 and NS059867 to G.W. Davis.

Submitted: 11 January 2011
Accepted: 22 August 2011

References

Akins, M.R., H.E. Berk-Rauch, and J.R. Fallon. 2009. Presynaptic translation: stepping out of the postsynaptic shadow. *Front Neural Circuits*. 3:17. http://dx.doi.org/10.3389/neuro.04.017.2009

Albin, S.D., and G.W. Davis. 2004. Coordinating structural and functional synapse development: postsynaptic p21-activated kinase independently specifies glutamate receptor abundance and postsynaptic morphology. *J. Neurosci.* 24:6871–6879. http://dx.doi.org/10.1523/JNEUROSCI.1538-04.2004

Antion, M.D., M. Merhav, C.A. Hoeffer, G. Reis, S.C. Kozma, G. Thomas, E.M. Schuman, K. Rosenblum, and E. Klann. 2008. Removal of S6K1 and S6K2 leads to divergent alterations in learning, memory, and synaptic plasticity. *Learn. Mem.* 15:29–38. http://dx.doi.org/10.1101/lm.661908

Atwood, H.L., C.K. Govind, and C.F. Wu. 1993. Differential ultrastructure of synaptic terminals on ventral longitudinal abdominal muscles in *Drosophila* larvae. *J. Neurobiol.* 24:1008–1024. http://dx.doi.org/10.1002/neu.480240803

Barcelo, H., and M.J. Stewart. 2002. Altering *Drosophila* S6 kinase activity is consistent with a role for S6 kinase in growth. *Genesis*. 34:83–85. http://dx.doi.org/10.1002/gene.10132

Bergquist, S., D.K. Dickman, and G.W. Davis. 2010. A hierarchy of cell intrinsic and target-derived homeostatic signaling. *Neuron*. 66:220–234. http://dx.doi.org/10.1016/j.neuron.2010.03.023

Biondi, R.M. 2004. Phosphoinositide-dependent protein kinase 1, a sensor of protein conformation. *Trends Biochem. Sci.* 29:136–142. http://dx.doi.org/10.1016/j.tibs.2004.01.005

Boylan, K.L., S. Mische, M. Li, G. Marqués, X. Morin, W. Chia, and T.S. Hays. 2008. Motility screen identifies *Drosophila* IGF-II mRNA-binding protein—zipcode-binding protein acting in oogenesis and synaptogenesis. *PLoS Genet.* 4:e36. http://dx.doi.org/10.1371/journal.pgen.0040036

Buckmaster, P.S., E.A. Ingram, and X. Wen. 2009. Inhibition of the mammalian target of rapamycin signaling pathway suppresses dentate granule cell axon sprouting in a rodent model of temporal lobe epilepsy. *J. Neurosci.* 29:8259–8269. http://dx.doi.org/10.1523/JNEUROSCI.4179-08.2009

Budnik, V., Y.H. Koh, B. Guan, B. Hartmann, C. Hough, D. Woods, and M. Gorczyca. 1996. Regulation of synapse structure and function by the *Drosophila* tumor suppressor gene dlg. *Neuron*. 17:627–640. http://dx.doi.org/10.1016/S0896-6273(00)80196-8

Burnett, P.E., S. Blackshaw, M.M. Lai, I.A. Qureshi, A.F. Burnett, D.M. Sabatini, and S.H. Snyder. 1998. Neurabin is a synaptic protein linking p70 S6 kinase and the neuronal cytoskeleton. *Proc. Natl. Acad. Sci. USA*. 95:8351–8356. http://dx.doi.org/10.1073/pnas.95.14.8351

Cammalleri, M., R. Lütjens, F. Berton, A.R. King, C. Simpson, W. Francesconi, and P.P. Sanna. 2003. Time-restricted role for dendritic activation of the mTOR-p70S6K pathway in the induction of late-phase long-term potentiation in the CA1. *Proc. Natl. Acad. Sci. USA*. 100:14368–14373. http://dx.doi.org/10.1073/pnas.2336098100

Colón-Ramos, D.A., M.A. Margeta, and K. Shen. 2007. Glia promote local synaptogenesis through UNC-6 (netrin) signaling in *C. elegans*. *Science*. 318:103–106. http://dx.doi.org/10.1126/science.1143762

Dai, Y., H. Taru, S.L. Deken, B. Grill, B. Ackley, M.L. Nonet, and Y. Jin. 2006. SYD-2 Liprin-alpha organizes presynaptic active zone formation through ELKS. *Nat. Neurosci.* 9:1479–1487. http://dx.doi.org/10.1038/nn1808

Dennis, P.B., N. Pullen, R.B. Pearson, S.C. Kozma, and G. Thomas. 1998. Phosphorylation sites in the autoinhibitory domain participate in p70(s6k) activation loop phosphorylation. *J. Biol. Chem.* 273:14845–14852. http://dx.doi.org/10.1074/jbc.273.24.14845

Dickman, D.K., and G.W. Davis. 2009. The schizophrenia susceptibility gene dysbindin controls synaptic homeostasis. *Science*. 326:1127–1130. http://dx.doi.org/10.1126/science.1179685

Fouquet, W., D. Owald, C. Wichmann, S. Mertel, H. Depner, M. Dyba, S. Hallermann, R.J. Kittel, S. Eimer, and S.J. Sigrist. 2009. Maturation of active zone assembly by *Drosophila* Bruchpilot. *J. Cell Biol.* 186:129–145.

Frank, C.A., M.J. Kennedy, C.P. Goold, K.W. Marek, and G.W. Davis. 2006. Mechanisms underlying the rapid induction and sustained expression of synaptic homeostasis. *Neuron*. 52:663–677. http://dx.doi.org/10.1016/j.neuron.2006.09.029

Frank, C.A., J. Pielage, and G.W. Davis. 2009. A presynaptic homeostatic signaling system composed of the Eph receptor, ephexin, Cdc42, and CaV2.1 calcium channels. *Neuron*. 61:556–569. http://dx.doi.org/10.1016/j.neuron.2008.12.028

Graf, E.R., R.W. Daniels, R.W. Burgess, T.L. Schwarz, and A. DiAntonio. 2009. Rab3 dynamically controls protein composition at active zones. *Neuron*. 64:663–677. http://dx.doi.org/10.1016/j.neuron.2009.11.002

Hill, A.A., D.H. Edwards, and R.K. Murphey. 1994. The effect of neuronal growth on synaptic integration. *J. Comput. Neurosci.* 1:239–254. http://dx.doi.org/10.1007/BF00961736

Howlett, E., C.C. Lin, W. Lavery, and M. Stern. 2008. A PI3-kinase-mediated negative feedback regulates neuronal excitability. *PLoS Genet.* 4:e1000277. http://dx.doi.org/10.1371/journal.pgen.1000277

Jaworski, J., S. Spangler, D.P. Seeburg, C.C. Hoogenraad, and M. Sheng. 2005. Control of dendritic arborization by the phosphoinositide-3′-kinase-Akt-mammalian target of rapamycin pathway. *J. Neurosci.* 25:11300–11312. http://dx.doi.org/10.1523/JNEUROSCI.2270-05.2005

Johnson, E.L. III, R.D. Fetter, and G.W. Davis. 2009. Negative regulation of active zone assembly by a newly identified SR protein kinase. *PLoS Biol.* 7:e1000193. http://dx.doi.org/10.1371/journal.pbio.1000193

Kaufmann, N., J. DeProto, R. Ranjan, H. Wan, and D. Van Vactor. 2002. *Drosophila* liprin-alpha and the receptor phosphatase Dlar control synapse morphogenesis. *Neuron*. 34:27–38. http://dx.doi.org/10.1016/S0896-6273(02)00643-8

Khan, A., A.M. Pepio, and W.S. Sossin. 2001. Serotonin activates S6 kinase in a rapamycin-sensitive manner in Aplysia synaptosomes. *J. Neurosci.* 21:382–391.

Kittel, R.J., C. Wichmann, T.M. Rasse, W. Fouquet, M. Schmidt, A. Schmid, D.A. Wagh, C. Pawlu, R.R. Kellner, K.I. Willig, et al. 2006. Bruchpilot promotes active zone assembly, Ca2+ channel clustering, and vesicle release. *Science*. 312:1051–1054. http://dx.doi.org/10.1126/science.1126308

Knox, S., H. Ge, B.D. Dimitroff, Y. Ren, K.A. Howe, A.M. Arsham, M.C. Easterday, T.P. Neufeld, M.B. O'Connor, and S.B. Selleck. 2007. Mechanisms of TSC-mediated control of synapse assembly and axon guidance. *PLoS ONE*. 2:e375. http://dx.doi.org/10.1371/journal.pone.0000375

Lin, D.M., and C.S. Goodman. 1994. Ectopic and increased expression of Fasciclin II alters motoneuron growth cone guidance. *Neuron*. 13:507–523. http://dx.doi.org/10.1016/0896-6273(94)90022-1

Marie, B., S.T. Sweeney, K.E. Poskanzer, J. Roos, R.B. Kelly, and G.W. Davis. 2004. Dap160/intersectin scaffolds the periactive zone to achieve high-fidelity endocytosis and normal synaptic growth. *Neuron*. 43:207–219. http://dx.doi.org/10.1016/j.neuron.2004.07.001

Marie, B., E. Pym, S. Bergquist, and G.W. Davis. 2010. Synaptic homeostasis is consolidated by the cell fate gene gooseberry, a *Drosophila* pax3/7 homolog. *J. Neurosci.* 30:8071–8082. http://dx.doi.org/10.1523/JNEUROSCI.5467-09.2010

Marqués, G., H. Bao, T.E. Haerry, M.J. Shimell, P. Duchek, B. Zhang, and M.B. O'Connor. 2002. The *Drosophila* BMP type II receptor Wishful Thinking regulates neuromuscular synapse morphology and function. *Neuron*. 33:529–543. http://dx.doi.org/10.1016/S0896-6273(02)00595-0

Marrus, S.B., S.L. Portman, M.J. Allen, K.G. Moffat, and A. DiAntonio. 2004. Differential localization of glutamate receptor subunits at the *Drosophila* neuromuscular junction. *J. Neurosci.* 24:1406–1415. http://dx.doi.org/10.1523/JNEUROSCI.1575-03.2004

McCabe, B.D., G. Marqués, A.P. Haghighi, R.D. Fetter, M.L. Crotty, T.E. Haerry, C.S. Goodman, and M.B. O'Connor. 2003. The BMP homolog Gbb provides a retrograde signal that regulates synaptic growth at the *Drosophila* neuromuscular junction. *Neuron*. 39:241–254. http://dx.doi.org/10.1016/S0896-6273(03)00426-4

Mee, C.J., E.C. Pym, K.G. Moffat, and R.A. Baines. 2004. Regulation of neuronal excitability through pumilio-dependent control of a sodium channel gene. *J. Neurosci.* 24:8695–8703. http://dx.doi.org/10.1523/JNEUROSCI.2282-04.2004

Menon, K.P., S. Sanyal, Y. Habara, R. Sanchez, R.P. Wharton, M. Ramaswami, and K. Zinn. 2004. The translational repressor Pumilio regulates presynaptic morphology and controls postsynaptic accumulation of translation factor eIF-4E. *Neuron*. 44:663–676. http://dx.doi.org/10.1016/j.neuron.2004.10.028

Menon, K.P., S. Andrews, M. Murthy, E.R. Gavis, and K. Zinn. 2009. The translational repressors Nanos and Pumilio have divergent effects on presynaptic terminal growth and postsynaptic glutamate receptor subunit composition. *J. Neurosci.* 29:5558–5572. http://dx.doi.org/10.1523/JNEUROSCI.0520-09.2009

Miech, C., H.U. Pauer, X. He, and T.L. Schwarz. 2008. Presynaptic local signaling by a canonical wingless pathway regulates development of the *Drosophila* neuromuscular junction. *J. Neurosci.* 28:10875–10884. http://dx.doi.org/10.1523/JNEUROSCI.0164-08.2008

Montagne, J., M.J. Stewart, H. Stocker, E. Hafen, S.C. Kozma, and G. Thomas. 1999. *Drosophila* S6 kinase: a regulator of cell size. *Science*. 285:2126–2129. http://dx.doi.org/10.1126/science.285.5436.2126

Mora, A., D. Komander, D.M. van Aalten, and D.R. Alessi. 2004. PDK1, the master regulator of AGC kinase signal transduction. *Semin. Cell Dev. Biol.* 15:161–170. http://dx.doi.org/10.1016/j.semcdb.2003.12.022

Nguyen, M., S. Park, G. Marqués, and K. Arora. 1998. Interpretation of a BMP activity gradient in *Drosophila* embryos depends on synergistic signaling by two type I receptors, SAX and TKV. *Cell*. 95:495–506. http://dx.doi.org/10.1016/S0092-8674(00)81617-7

Oliver, C.J., R.T. Terry-Lorenzo, E. Elliott, W.A. Bloomer, S. Li, D.L. Brautigan, R.J. Colbran, and S. Shenolikar. 2002. Targeting protein phosphatase 1 (PP1) to the actin cytoskeleton: the neurabin I/PP1 complex regulates cell morphology. *Mol. Cell. Biol.* 22:4690–4701. http://dx.doi.org/10.1128/MCB.22.13.4690-4701.2002

Packard, M., E.S. Koo, M. Gorczyca, J. Sharpe, S. Cumberledge, and V. Budnik. 2002. The *Drosophila* Wnt, wingless, provides an essential signal for pre- and postsynaptic differentiation. *Cell*. 111:319–330. http://dx.doi.org/10.1016/S0092-8674(02)01047-4

Patel, M.R., and K. Shen. 2009. RSY-1 is a local inhibitor of presynaptic assembly in *C. elegans*. *Science*. 323:1500–1503. http://dx.doi.org/10.1126/science.1169025

Pielage, J., R.D. Fetter, and G.W. Davis. 2006. A postsynaptic spectrin scaffold defines active zone size, spacing, and efficacy at the *Drosophila* neuromuscular junction. *J. Cell Biol.* 175:491–503. http://dx.doi.org/10.1083/jcb.200607036

Pielage, J., L. Cheng, R.D. Fetter, P.M. Carlton, J.W. Sedat, and G.W. Davis. 2008. A presynaptic giant ankyrin stabilizes the NMJ through regulation of presynaptic microtubules and transsynaptic cell adhesion. *Neuron*. 58:195–209. http://dx.doi.org/10.1016/j.neuron.2008.02.017

Purves, D., and J.W. Lichtman. 1978. Formation and maintenance of synaptic connections in autonomic ganglia. *Physiol. Rev.* 58:821–862.

Radimerski, T., J. Montagne, F. Rintelen, H. Stocker, J. van der Kaay, C.P. Downes, E. Hafen, and G. Thomas. 2002. dS6K-regulated cell growth is dPKB/dPI(3)K-independent, but requires dPDK1. *Nat. Cell Biol.* 4:251–255. http://dx.doi.org/10.1038/ncb763

Rintelen, F., H. Stocker, G. Thomas, and E. Hafen. 2001. PDK1 regulates growth through Akt and S6K in *Drosophila*. *Proc. Natl. Acad. Sci. USA*. 98:15020–15025. http://dx.doi.org/10.1073/pnas.011318098

Roos, J., T. Hummel, N. Ng, C. Klämbt, and G.W. Davis. 2000. *Drosophila* Futsch regulates synaptic microtubule organization and is necessary for synaptic growth. *Neuron*. 26:371–382. http://dx.doi.org/10.1016/S0896-6273(00)81170-8

Ryan, X.P., J. Alldritt, P. Svenningsson, P.B. Allen, G.Y. Wu, A.C. Nairn, and P. Greengard. 2005. The Rho-specific GEF Lfc interacts with neurabin and spinophilin to regulate dendritic spine morphology. *Neuron*. 47:85–100. http://dx.doi.org/10.1016/j.neuron.2005.05.013

Shen, K., and C.I. Bargmann. 2003. The immunoglobulin superfamily protein SYG-1 determines the location of specific synapses in *C. elegans*. *Cell*. 112:619–630. http://dx.doi.org/10.1016/S0092-8674(03)00113-2

Shen, W., and B. Ganetzky. 2009. Autophagy promotes synapse development in *Drosophila*. *J. Cell Biol.* 187:71–79. http://dx.doi.org/10.1083/jcb.200907109

Sherwood, N.T., Q. Sun, M. Xue, B. Zhang, and K. Zinn. 2004. *Drosophila* spastin regulates synaptic microtubule networks and is required for normal motor function. *PLoS Biol.* 2:e429. http://dx.doi.org/10.1371/journal.pbio.0020429

Sieburth, D., Q. Ch'ng, M. Dybbs, M. Tavazoie, S. Kennedy, D. Wang, D. Dupuy, J.F. Rual, D.E. Hill, M. Vidal, et al. 2005. Systematic analysis of genes required for synapse structure and function. *Nature*. 436:510–517. http://dx.doi.org/10.1038/nature03809

Sweeney, S.T., and G.W. Davis. 2002. Unrestricted synaptic growth in spinster-a late endosomal protein implicated in TGF-beta-mediated synaptic growth regulation. *Neuron*. 36:403–416. http://dx.doi.org/10.1016/S0896-6273(02)01014-0

Terry-Lorenzo, R.T., D.W. Roadcap, T. Otsuka, T.A. Blanpied, P.L. Zamorano, C.C. Garner, S. Shenolikar, and M.D. Ehlers. 2005. Neurabin/protein phosphatase-1 complex regulates dendritic spine morphogenesis and maturation. *Mol. Biol. Cell*. 16:2349–2362. http://dx.doi.org/10.1091/mbc.E04-12-1054

Wagh, D.A., T.M. Rasse, E. Asan, A. Hofbauer, I. Schwenkert, H. Dürrbeck, S. Buchner, M.C. Dabauvalle, M. Schmidt, G. Qin, et al. 2006. Bruchpilot, a protein with homology to ELKS/CAST, is required for structural integrity and function of synaptic active zones in *Drosophila*. *Neuron*. 49:833–844. http://dx.doi.org/10.1016/j.neuron.2006.02.008

Wairkar, Y.P., H. Toda, H. Mochizuki, K. Furukubo-Tokunaga, T. Tomoda, and A. DiAntonio. 2009. Unc-51 controls active zone density and protein composition by downregulating ERK signaling. *J. Neurosci.* 29:517–528. http://dx.doi.org/10.1523/JNEUROSCI.3848-08.2009

Wan, H.I., A. DiAntonio, R.D. Fetter, K. Bergstrom, R. Strauss, and C.S. Goodman. 2000. Highwire regulates synaptic growth in *Drosophila*. *Neuron*. 26:313–329. http://dx.doi.org/10.1016/S0896-6273(00)81166-6

Weatherill, D.B., J. Dyer, and W.S. Sossin. 2010. Ribosomal protein S6 kinase is a critical downstream effector of the target of rapamycin complex 1 for long-term facilitation in Aplysia. *J. Biol. Chem.* 285:12255–12267. http://dx.doi.org/10.1074/jbc.M109.071142